



Molecular interaction between SH3 domain of PACSIN2 and proline-rich motifs of Cobll1

Hee-Seop Yoo^{1,2,†}, Seung-Hyeon Seok^{3,†}, Ha-Neul Kim^{1,2}, Ji-Hun Kim^{4,*}, and Min-Duk Seo^{1,2,*}

¹Department of Molecular Science and Technology, Ajou University, Suwon, Gyeonggi 16499, Republic of Korea
²College of Pharmacy and Research Institute of Pharmaceutical Science and Technology (RIPST), Ajou University, Suwon, Gyeonggi 16499, Republic of Korea

³College of Pharmacy and Interdisciplinary Graduate Program in Advanced Convergence Technology & Science, Jeju National University, Jeju, Jeju 63243, Republic of Korea

⁴College of Pharmacy, Chungbuk National University, Cheongju, Chungbuk 28160, Republic of Korea

Received Sep 13, 2022; Revised Sep 16, 2022; Accepted Sep 16, 2022

Abstract The SH3 domain found within a variety of proteins is comprised of generally 60 residues, and participated in protein-protein interactions with proline-rich motifs. Cobll1 was identified as a distinct molecular marker associated with CML progression, and PACSIN2 was discovered a novel Cobll1 binding partner through direct interaction between a SH3 domain of PACSIN2 and three proline-rich motifs of Cobll1. To understand the structural basis of interactions between PACSIN2 and Cobll1, backbone assignments of PACSIN2 SH3 domain were performed. Furthermore, three proline-rich peptides of Cobll1 were titrated to ¹⁵N-labeled PACSIN2 SH3 domain in various ratios. Our chemical shift changes data and conserved SH3 sequence alignment will be helpful to analyze fundamental molecular basis related to the interaction between PACSIN2 and Cobll1.

Keywords Cobll1, PACSIN2, proline-rich motif, SH3 domain, chronic myeloid Leukemia

Introduction

Chronic myeloid leukemia (CML) is a malignant hematopoietic disorder¹ caused by the genetic lesion of chromosomes 9 and 22 harboring the BCR-ABL oncogene.² This myeloproliferative disorder progresses three distinct clinical phases: chronic phase, accelerated phase, and blast crisis.³

Since imatinib, the first BCR-ABL1 tyrosine kinase inhibitor (TKI), was approved in 2001, TKIs have been considered the standard treatment for CML.⁴ However, imatinib and potent next-generation TKIs have exhibited drug resistance in some patients during blast crisis progression.^{5,6,7}

Cordon-bleu protein-like 1 (Cobll1) is reported as a negative regulator of apoptosis in tumor cells and associated with various cancer and metabolic diseases.^{8,9,10,11} In addition, high-level expression of Cobll1 is associated with the TKI resistance and blast transformation in CML.¹² PACSIN2 is a ubiquitously expressed cytoplasmic protein consisting of an N-terminal F-BAR domain and a C-terminal Src homology 3 (SH3) domain.^{13,14} In addition to the basic functions, including cellular migration and signaling, PACSIN2 plays an essential role for inducing apoptosis with TKI treatment.^{13,14,15} Cobll1 binds to PACSIN2 through three proline-rich motifs (PRMs)

*Address correspondence to: **Min-Duk Seo**, Department of Molecular Science and Technology, Ajou University, Suwon, Gyeonggi 16499, Republic of Korea, Tel: 82-31-219-3450; E-mail: mdseo@ajou.ac.kr; **Ji-Hun Kim**, College of Pharmacy, Chungbuk National University, Cheongju, Chungbuk 28160, Republic of Korea, Tel: 82-43-249-1343; E-mail: nmrjkhkim@cbnu.ac.kr

†These authors are contributed equally to this work.

of Cobll1 and the SH3 domain of PACSIN2, and this interaction consequently leads to the resistance of TKIs.¹⁵ To investigate the role of each PRMs of Cobll1 for PACSIN2 SH3 domain, we performed backbone resonance assignments of PACSIN2 SH3 domain and NMR titration experiments with the peptides corresponding the three PRMs of Cobll1. Our studies reveal that overall binding mode of each Cobll1 PRMs to PACSIN2 SH3 domain is similar although the chemical environments induced by the binding are slightly different.

Experimental Methods

Sample preparation – Preparation of PACSIN2 SH3 domain was performed as described previously.¹⁵ Briefly, the recombinant plasmid pGEX-4T-1 containing the SH3 domain of PACSIN2 (residues 430-486) was transformed into *E. coli* BL21-CodonPlus(DE3). Overexpression of protein was induced with 0.5 mM isopropyl β -D-1-thiogalactopyranoside (IPTG), and cells were harvested by centrifugation and disrupted by sonication in lysis buffer (20mM Tris-HCl, 500mM NaCl, 10% Glycerol, 0.2% Nonidet P-40 (NP40), 0.4 mM Tris(2-carboxyethyl)phosphine hydrochloride (TCEP), 1mM EDTA, pH 7.0). The proteins were purified by affinity chromatography with a GST column, and cleaved by thrombin to remove the GST fusion tag. The cleaved proteins were purified by ion exchange chromatography (Fractogel, MERCK), and further purification was performed using HiLoad 16/600 Superdex 75 prep grade column (GE Healthcare) in final buffer (50 mM sodium phosphate, 100 mM NaCl, 1 mM TCEP, pH 6.3).

NMR experiments – The [¹⁵N]- or [¹⁵N, ¹³C]-labeled PACSIN2 SH3 domain was expressed in M9 minimal media using ¹⁵N-enriched ammonium chloride and/or ¹³C-enriched glucose, and the proteins were purified with the same procedures as described above. Sequential assignment of ¹³C, ¹⁵N-labeled PACSIN2 SH3 domain was performed using 2D ¹H-¹⁵N heteronuclear single quantum correlation (HSQC) and 3D triple resonance experiments (HNCACB and

CBCACONH) recorded at 298K on a Bruker AVANCE II 600 MHz spectrometer. All ¹H-¹⁵N HSQC NMR titrations were performed at 298K on a Bruker AVANCE II 800 MHz spectrometer. Three proline-rich peptides derived from Cobll1 (AKAPLPPAETK, 1st proline-rich peptide; RRAPLPPMPAS, 2nd proline-rich peptide; RKAPSPPSKIP, 3rd proline-rich peptide) were synthesized, and dissolved in the final buffer with concentrations of 9 mM. The 2nd proline-rich peptide was titrated to the 100 μ M of ¹⁵N-labeled PACSIN2 SH3 domain in various molar ratios (PACSIN2 SH3 domain:2nd proline-rich peptide=1:0, 1:0.25, 1:0.5, 1:1, 1:2, 1:3, and 1:4). The molar ratios of PACSIN2 SH3 domain: 1st or 3rd proline-rich peptides was as follows; 1:0, 1:0.25, 1:0.5, 1:1, 1:2, 1:3, 1:4, and 1:8. The chemical shift perturbations (CSPs) were calculated using following equation: $CSP (\Delta\delta_{H,N}) = \sqrt{((\Delta\delta_H)^2 + \frac{1}{6}(\Delta\delta_N)^2)}$ where $\Delta\delta_H$ and $\Delta\delta_N$ are the amide proton and nitrogen chemical shift differences, respectively. All spectra were processed using NMRpipe and visualized using NMRViewJ software.

Results and Discussion

Backbone assignment of PACSIN2 SH3 domain – The backbone amide (¹H and ¹⁵N) resonances of PACSIN2 SH3 domain were completely assigned by heteronuclear triple resonance NMR spectroscopy. Backbone assignments were carried out 60 of 62 residues (96%), except 1 proline and unobserved residue (H442) in the ¹H-¹⁵N HSQC spectrum (Figure 1). The backbone chemical shifts of PACSIN2 SH3 domain are listed in Table 1.

Interaction between PACSIN2 SH3 domain and proline-rich motifs of Cobll1 – The peptides corresponding the three proline-rich motifs (i.e., residues 18-25, 292-299, 361-368) of Cobll1 were synthesized, and each peptide was added to ¹⁵N-labeled PACSIN2 SH3 domain with various molar ratios. As shown in Figure 2, many residues of PACSIN2 SH3 domain were affected upon addition of proline-rich peptides derived from Cobll1. Several

residues of PACSIN2 SH3 domain, including Y437, Q440, E441, D460, G463, A479, N480, V482, and A484, were commonly perturbed by each of the three proline-rich peptides, albeit much weaker perturbation by the first proline-rich peptide (residues 18-25). Average chemical shift perturbations (CSP, $\Delta\delta$) for PACSIN2 SH3 domain on binding to each peptide were plotted in Figure 3. These results suggest that although the chemical environments induced by binding of each proline-rich motifs of Cobll1 are different, the overall binding mode of each of three proline-rich motifs of Cobll1 to PACSIN2 SH3 domain are similar (Figure 2). These results reveal that Cobll1 strongly binds to the SH3 domain of PACSIN2 through its proline-rich motifs (Figure 2).

Sequence alignment of PACSIN2 SH3 domain with other conserved SH3 domains – As shown in Figure 4, the sequence of PACSIN2 SH3 domain is aligned with other SH3 domains. The SH3 domain typically has five β -strands which are structurally and sequentially conserved, and these β -strands are connected with RT loop, n-Src loop, distal loop, and 3¹⁰ helix, respectively (Figure 4).¹⁶ The well-conserved key aromatic and acidic residues (Y435, Y437, D443, E444, W464, P478, and Y481) of PACSIN2 SH3 are necessary for the interaction with canonical PxxP motif. Based on our CSP analysis and sequence alignment, we suggested that proline-rich peptides derived from Cobll1 binds to the classic proline binding groove of PACSIN2 SH3 domain.

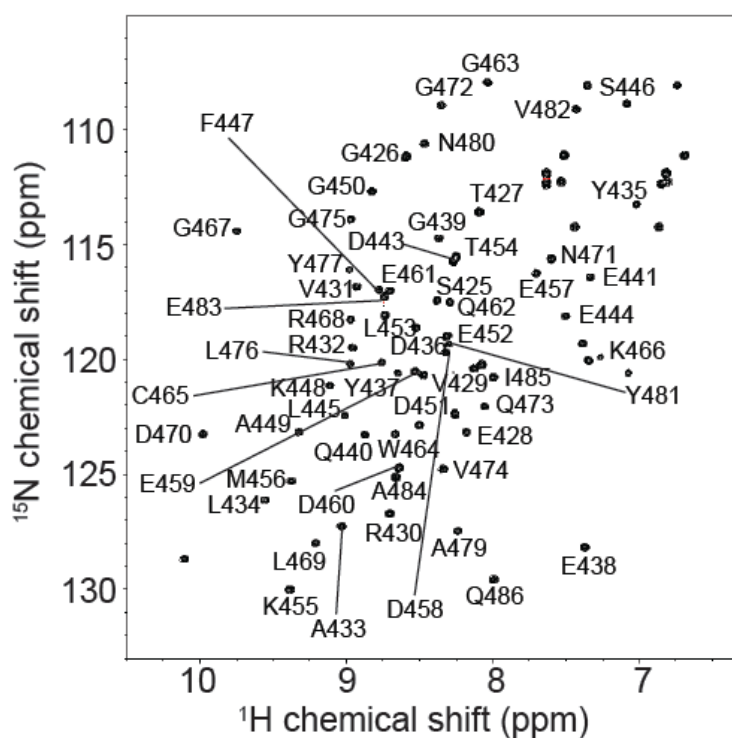


Figure 1. ^1H - ^{15}N HSQC spectra of ^{15}N -labelled PACSIN SH3 domain. The backbone amide cross peaks are annotated by residue names and numbers.

Table 1. Backbone ^1HN , ^{15}N , $^{13}\text{C}_\alpha$, $^{13}\text{C}_\beta$ chemical shifts of PACSIN SH3 domain (unit:ppm)

Residue	^1HN	^{15}N	$^{13}\text{C}_\alpha$	$^{13}\text{C}_\beta$	Residue	^1HN	^{15}N	$^{13}\text{C}_\alpha$	$^{13}\text{C}_\beta$
425 SER	8.38	117.46	58.56	64.01	456 MET	9.38	125.31		36.09
426 GLY	8.59	111.18	45.64		457 GLU	7.70	116.27		34.17
427 THR	8.09	113.6	61.81	69.66	458 ASP	8.32	119.70	58.5	40.05
428 GLU	8.18	123.17	56.61	30.68	459 GLU	8.53	120.53	56.53	30.77
429 VAL	8.13	120.39	61.11	35.37	460 ASP	8.64	124.72	52.48	41.29
430 ARG	8.70	126.71	55.04	30.94	461 GLU	8.70	117.01	58.74	29.31
431 VAL	8.93	116.83	58.76	35.83	462 GLN	8.30	117.52	55.74	
432 ARG	8.96	119.5	53.25	33.92	463 GLY	8.04	107.96	45.51	
433 ALA	9.03	127.25	52.42	20.13	464 TRP	8.67	123.25	56.71	30.75
434 LEU	9.56	126.12	55.54	43.38	465 CYS	8.76	120.12	57.72	
435 TYR	7.02	113.27	54.1	42.46	466 LYS	7.27	119.91	55.45	34.81
436 ASP	8.53	118.63	54.66	41.39	467 GLY	9.75	114.43	45.22	
437 TYR	8.65	120.58	59.2	42.24	468 ARG	8.97	118.28	53.79	34.83
438 GLU	7.37	128.18	53.64	30.16	469 LEU	9.21	127.99		
439 GLY	8.37	114.73	46.86		470 ASP	9.98	123.25	57.1	39.2
440 GLN	8.87	123.29	55.89	30.75	471 ASN	7.60	115.63	52.86	41.11
441 GLU	7.33	116.43	54.38	32.24	472 GLY	8.35	108.94	44.8	
442 HIS					473 GLN	8.06	122.05	57.51	29.02
443 ASP	8.27	115.73	53.96	39.69	474 VAL	8.34	124.77	60.33	34.41
444 GLU	7.50	118.11	55.74	32.57	475 GLY	8.97	113.92	45.67	
445 LEU	9.01	122.45	54.41	44.94	476 LEU	8.98	120.19	54.09	45.1
446 SER	7.09	108.88	57.37	66.15	477 TYR	8.98	116.10	55.8	39.56
447 PHE	8.78	116.98	56.03	39.52	478 PRO				
448 LYS	9.11	121.14	53.16	34.66	479 ALA	8.24	127.47	55.23	19.79
449 ALA	9.33	123.16	53.86	18.01	480 ASN	8.47	110.62	54.63	38.85
450 GLY	8.83	112.69	44.93		481 TYR	8.31	119.36	56.03	37.18
451 ASP	8.50	122.86	55.52	40.96	482 VAL	7.43	109.12	58.55	35.75
452 GLU	8.31	118.98			483 GLU	8.74	117.32	53.46	33.49
453 LEU	8.73	118.08	55.39	43.02	484 ALA	8.66	125.14	48.78	26.08
454 THR	8.25	115.57	62.52	70.5	485 ILE	7.99	120.79	62	38.69
455 LYS	9.39	130.02	49.29	41.51	486 GLN	7.99	129.57	57.55	30.8

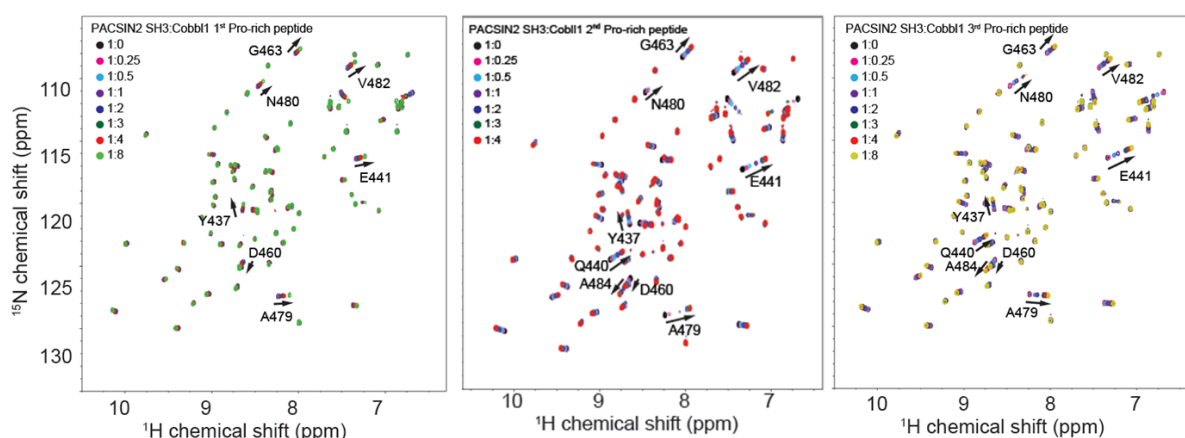


Figure 2. Overlay of ^1H - ^{15}N HSQC spectra of PACSIN2 SH3 domain in the presence of increasing concentrations of the peptides derived from Cobll1. The residues largely affected by Cobll1-derived peptides binding were marked, and arrows indicate the directions of chemical shift changes as the concentrations of the peptides increase.

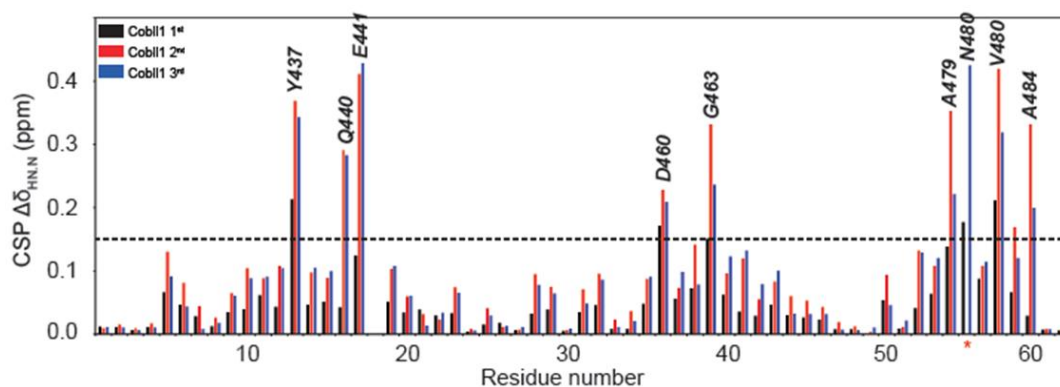


Figure 3. The values of chemical shift perturbation (CSP, $\Delta\delta_{\text{HN,N}}$) observed in ^1H - ^{15}N HSQC spectra of PACSIN2 SH3 upon binding with the saturated concentrations of three Cobll1 proline-rich peptides (PACSIN2 SH3 domain:proline-rich peptides=1:4). The nine residues showing the CSP values ($\Delta\delta_{\text{HN,N}}$) of upper 1.5 were indicated. The residue N56 disappeared upon Cobll1 2nd Pro-rich peptide binding, and indicated with the red asterisk.

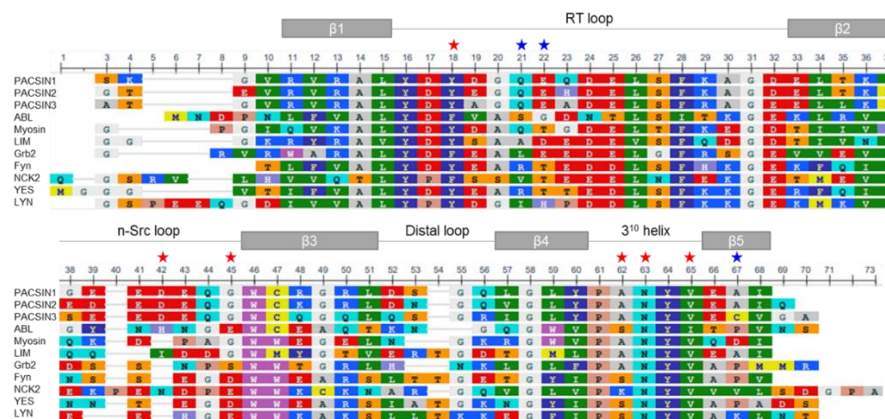


Figure 4. Sequence alignment of PACSIN2 with other SH3 domain containing proteins. Residues are also colored in respective sequences. The secondary structural elements are indicated above the sequence. Key residues highly affected by Cobll1 binding are indicated in asterisks, and red and blue asterisks indicate the highly and less conserved residues among SH3 domains, respectively.

Acknowledgements

This work was supported by grants from the Basic Science Research Program through the National Research Foundation (NRF) of Korea, funded by the Ministry of Education, Science and Technology (2020R1A2C3008889). The authors thank the high field NMR facility at the Korea Basic Science Institute

References

1. B. Chereda and J. V. Melo, *Ann. Hematol.* **94**, (2015)
2. F. Stefan, T. Moshe, E. Zeev, O. Susan, K. Razelle, and M. K. Hagop, *N. Engl. J. Med.* **341**, (1999)
3. C. Bruno and P. Danilo, *Blood* **103**, 11 (2004)
4. J. Elias, *Am. J. Hematol.* **91**, 1 (2016)
5. P. S. Neil, T. Chris, Y. L. Francis, C. Ping, N. Derek and L. S. Charles, *Science* **305**, 5682 (2004)
6. A. E. Christopher, O. Thomas, *Curr. Hematol. Malig. Rep.* **10**, 2 (2015)
7. J. D. Brian, G. Francois, G. O. Stephen, G. Insa and A. L. Richard et al., *N. Engl. J. Med.* **355**, (2006)
8. T. Nagase, K. Ishikawa, M. Suyama, R. Kikuno, M. Hirosawa, N. Miyajima, A. Tanaka, H. Kotani, N. Nomura, O. Ohara, *DNA Res.* **6**, 1 (1999)
9. P. Hana, J. Pavlina, M. Archana, S. Lucie, P. Lucie, L. Antonin, P. Karla, O. Petra, R. Lenka, D. Michael, P. Sarka, P. Sarka and B. Vitezslav, *Haematologica* **103**, 2 (2018)
10. T. Kenichi, S. Takashi, F. Tetsuya and I. Satoshi, *Proc. Natl. Acad. Sci. U.S.A.* **115**, 19 (2018)
11. U. Przemyslaw, M. Damian, C. Michal, S. Krzysztof, T. Maciej, D. Violetta and P. Andrzej, *Biomedicines* **10**, 8 (2022)
12. S. H. Han, S. K. Kim, H. J. Kim, Y. Lee, S. Y. Choi, G. Park, D. H. Kim, A. Lee, J. Kim, J. M. Choi, Y. Kim, K. Myung, H. Kim and D. W. Kim, *Leukemia* **31**, 7 (2017)
13. B. Ritter, J. Modregger, M. Paulsson and M. Plomann, *FEBS Lett.* **454**, 3, (1999)
14. S. M. Tsveta, A. U. Ana, N. Julian, T. Marina, M. S. Miesje, J. Vera, H. Annett, G. G. Anouk, T. Merel, G. Mariona, P. Markus and H. Stephan, *Nat. Commun.* **12**, 2610 (2021)
15. K. B. Park, H. S. Yoo, C. K. Oh, J. R. Lee, H. J. Chung, H. N. Kim, S. H. Kim, K. M. Kee, T. Y. Kim, M. S. Kim, B. H. Kim, J. S. Ra, K. J. Myung, H. T. Kim, S. H. Han, M. D. Seo, Y. S. Lee, D. W. Kim, *Cancer Med.* **10**, 1002 (2022)
16. N. Kurochkina and U. Guha, *Biophys Rev.* **5**, 1 (2012)